Variability of the focussed wind in Cyg X-1 / HDE 226868 system

Victoria Grinberg[1], N. Hell[2,3], M. Leutenegger[4,5], K. Pottschmidt[4,5], M. Hanke[2], I. Miškovičová[2], J. Wilms[2],
M. Böck[6], A. Bodaghee[7], G.V. Brown[3], M. Cadolle Bel[8], R. Duro[2], J. García[9], J. Lee[10], A. Lohfink[11], O.K. Madej[12,13], M.A. Nowak[1],
J. Rodriguez[14], N. Schulz[1], J. Sundqvist[8,15], J.A. Tomsick[16], R.H.D. Townsend[17]

[1]MIT, Cambridge, MA, USA - [2]Remeis-Observatory/ECAP/FAU, Bamberg, Germany - [3]LLNL, Livermore, CA, USA - [4]CRESST/NASA-GSFC, Greenbelt, MD, USA - [5]UMBC, Baltimore, MD, USA
[6]MPIfR, Bonn, Germany - [7]GCSU, Milledgeville, GA, USA - [8]LMU, Munich, Germany - [9]Harvard/CfA, Cambridge, MA, USA - [10]Harvard/SEAS, Cambridge, MA, USA - [11]University of Cambridge, Cambridge, UK -
[12]RU, Nijmegen, NL - [13]SRON, Utrecht, NL - [14]Lab. AIM, CEA-Saclay, France - [15]UD, Newark, DE, USA - [16]SSL, UC Berkeley, Berkeley, CA, USA - [15]UWM, Madison, WI, USA

contact: grinberg@space.mit.edu

15 years of Science with Chandra Symposium, November 18-21 2014, Boston, MA, USA

Abstract

Binary systems with a compact object are a unique chance to investigate the strong, clumpy winds of early type supergiants by using the compact object's X-rays as a probe of the wind structure. We analyze the two-component wind of HDE 226868, the O9.7Iab companion of the black hole Cyg X-1. Using *Chandra*-HETG we separate signatures of the hot gas phase from that due to additional absorption by the clumps and, using 5 hard state observations, study orbital variations and thus the spatial structure of the wind. Using $\sim$4.8 Ms of *RXTE* data we investigae the long-term orbital variability of the wind on 2 ks time scales throughout different accretion regimes of the black hole.
We review our results in the context of focused wind models and models for winds of O/B type stars.

Focussed clumpy wind in Cyg X-1 / HDE 226868 system

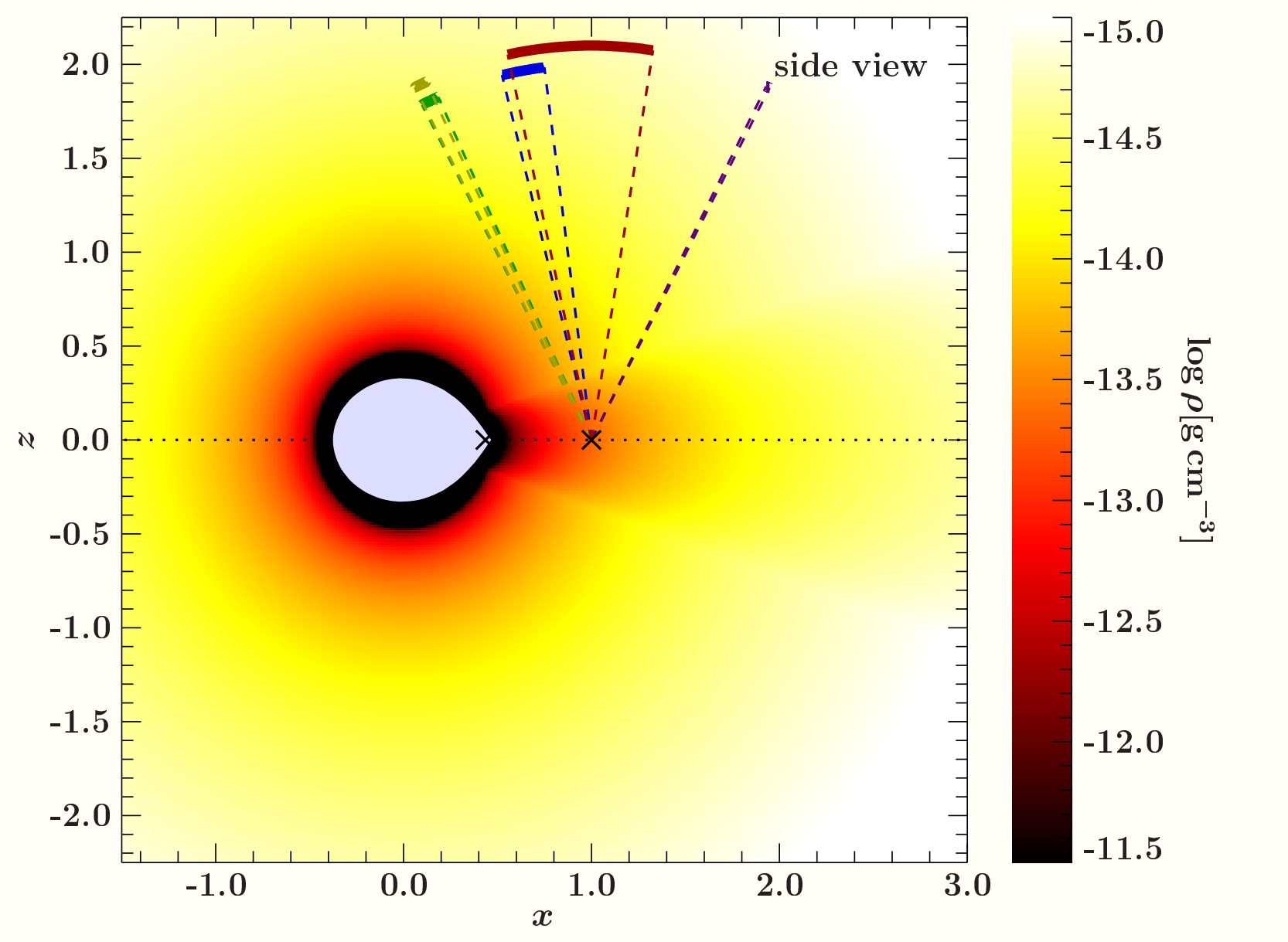

Given the system inclination of $\sim 30^\circ$, our line of sight probes different parts of the wind at different orbital phases. Additionally, the wind density and mass loss are enhanced along the binary axis. The left figure shows a density map of the focused wind model (Gies and Bolton, 1986), consisting of a line-driven CAK model (Castor et al., 1975) with longitudinal variation of wind parameters in a cone $\pm 20^\circ$ from the donor-BH line. Perturbation, i.e., variations of density, velocity, and temperature compress the gas in the stellar wind to small overdense structures, resulting in a two-component medium of cold clumps embedded in tenuous hot gas (Owocki et al. 1988; Feldmeier et al. 1997; Oskinova et al. 2012)
In the hard state (prominent power-law shape of the X-ray spectrum, low contribution from thermal component/accretion disk) we can use the X-rays from the vicinity of the black hole to investigate this wind. The lightcurves and hardness/softness ratios then show distinct absorption events, "dips", that correspond to passages of clumps through the line of sight (right figure, *Chandra* lightcurves). The dips are enhanced towards $\phi_\mathrm{orb} \approx 0$.

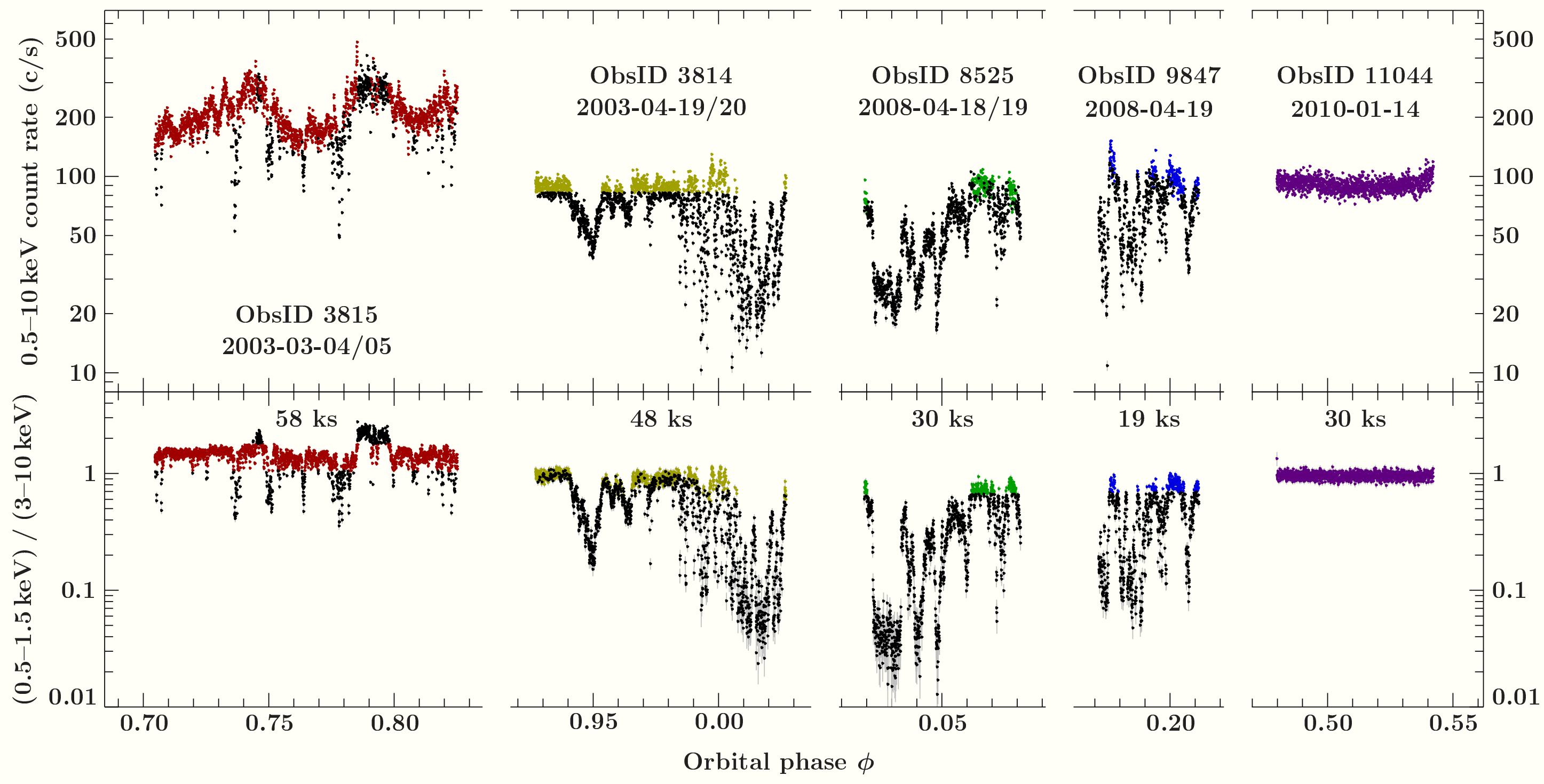

Long-term variability with RXTE (Grinberg et al., A&A to be subm.)

We use 2741 individual orbit-wise spectra of Cyg X-1 with an average exposure of $\sim$1.7 ks (total exposure $\sim$5 Ms) and model them following Wilms et al. (2006) and Grinberg et al. (2013,2014) with a broken power law model with a soft photon index Γ_1 modified by a cut-off and a Gaussian component at $\sim$6.4 keV. The absorption is modelled with `tbnew`, an improved version of `tbabs` (Wilms et al. 2000). To account for the ISM absorption towards the source we set the minimum value of the equivalent hydrogen column density to $N_\mathrm{H,ISM} = 4.8 \times 10^{21}\,\mathrm{cm}^{-2}$ (Xiang et al. 2011). To characterize the different accretion regimes, we use Γ_1-based state definitions derived in Grinberg et al. (2013) using spectral and timing properties: the source is in hard state if $\Gamma_1 \leq 2.0$, in the intermediate state if $2.0 < \Gamma_1 \leq 2.5$ and in the soft state if $2.5 < \Gamma_1$. In the intermediate and soft states, the absorption column cannot be constrained well because of the presence of a multitemperature disk component. There are signs of increasing absorption towards $\phi \approx 0$ in the intermediate state, but no variability is detectable in the soft state.

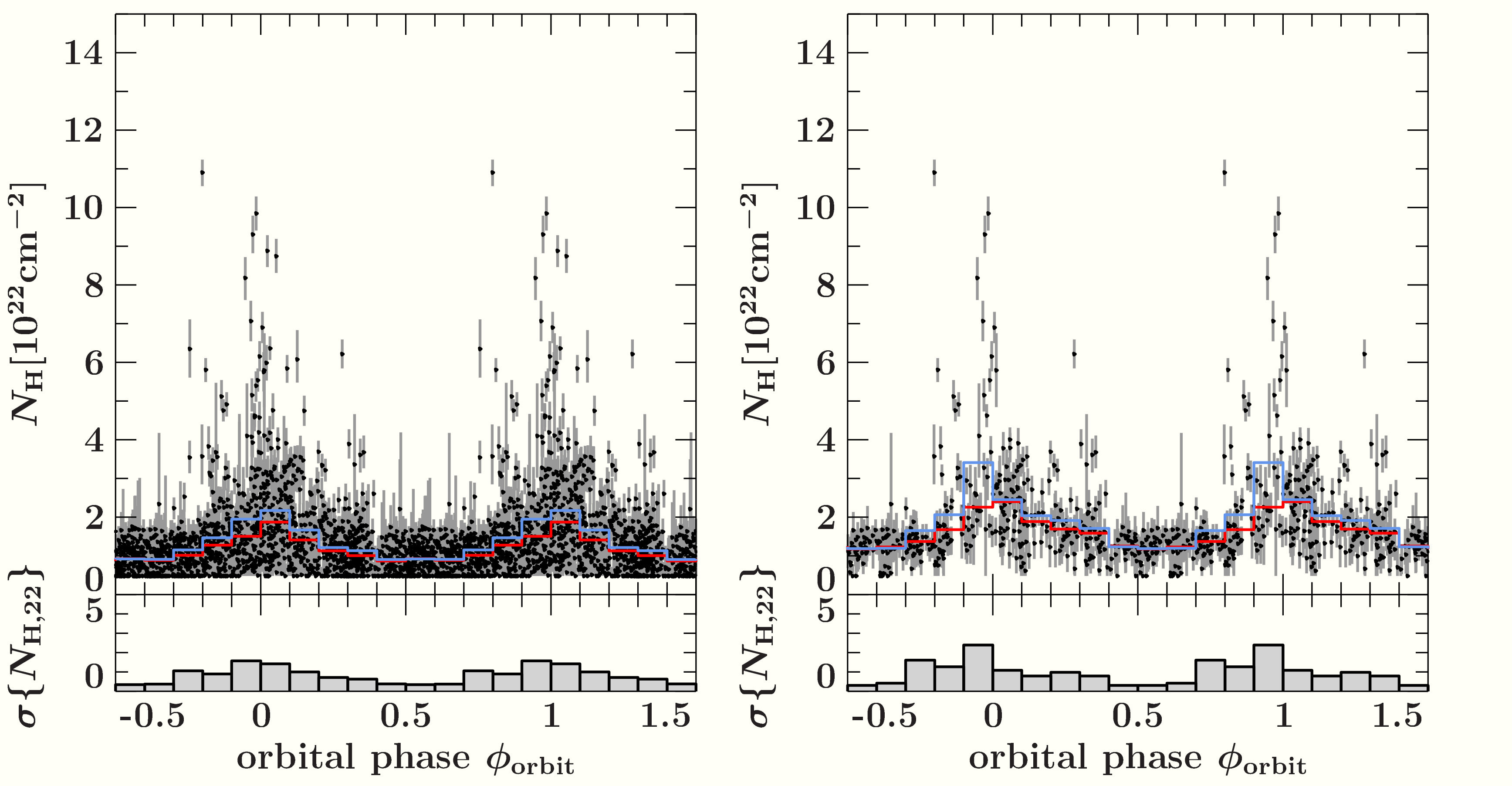

In the hard state, clear variability in both N_H and its standard deviation, $\sigma\{N_\mathrm{H,22}\} := \sigma\{N_\mathrm{H}/(10^{22}\,\mathrm{cm}^{-2})\}$ can be seen in the (left figure above; averages shown in blue, medians in red). This agrees with previous findings. The exceptional exposure reveals individual very deep absorption events ("dips"). Smooth focussed wind models cannot explain the observed variation of absorption at a given orbital phase.
Within the hard state, Cyg X-1 can display a range of spectral and timing behaviors (Pottschmidt et al. 2003; Wilms et al. 2006; Grinberg et al. 2014). At the same time, we expect the behavior of the absorption to depend on the broadband spectral shape of the X-rays because of the ionization of the wind. For a detailed analysis of absorption, we therefore need a hard state with stable spectral and timing characteristics, such as the long hard state of 2006-2010 (right figure above, see also Grinberg et al. 2013).

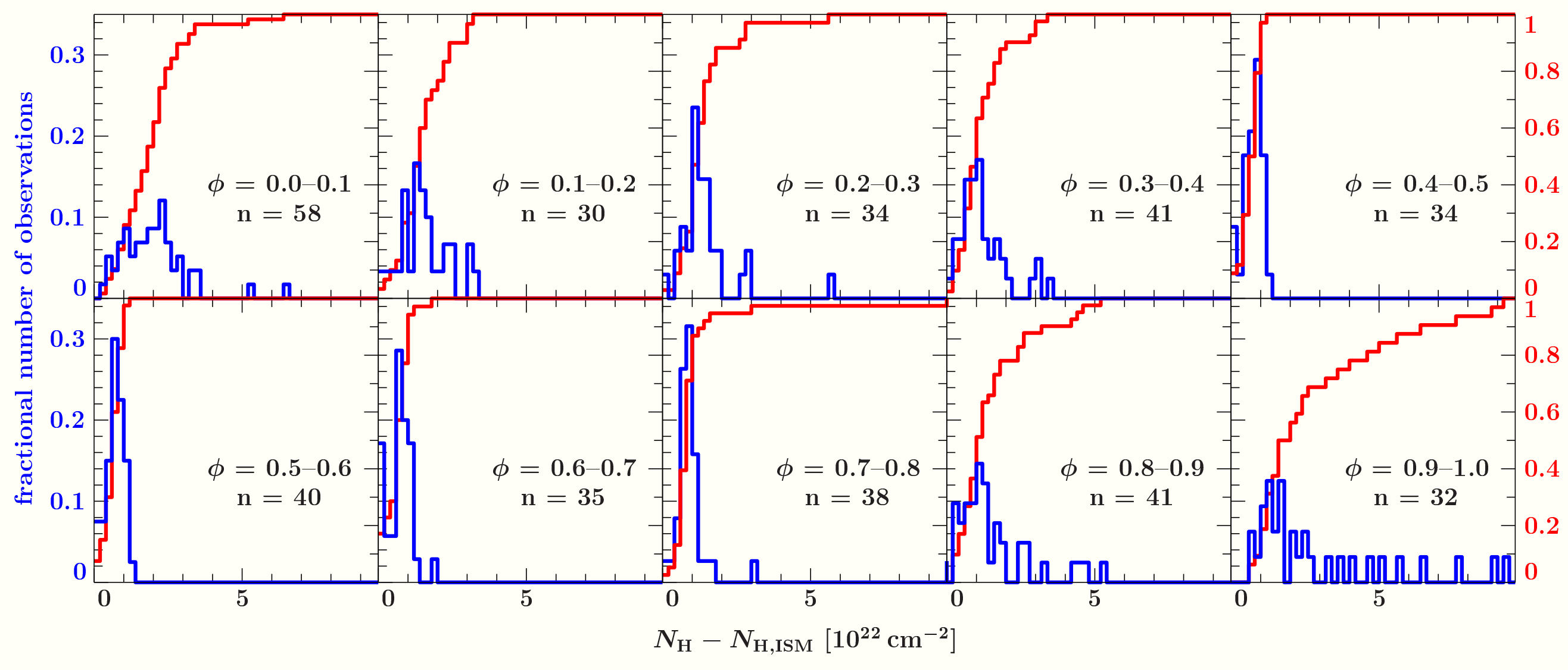

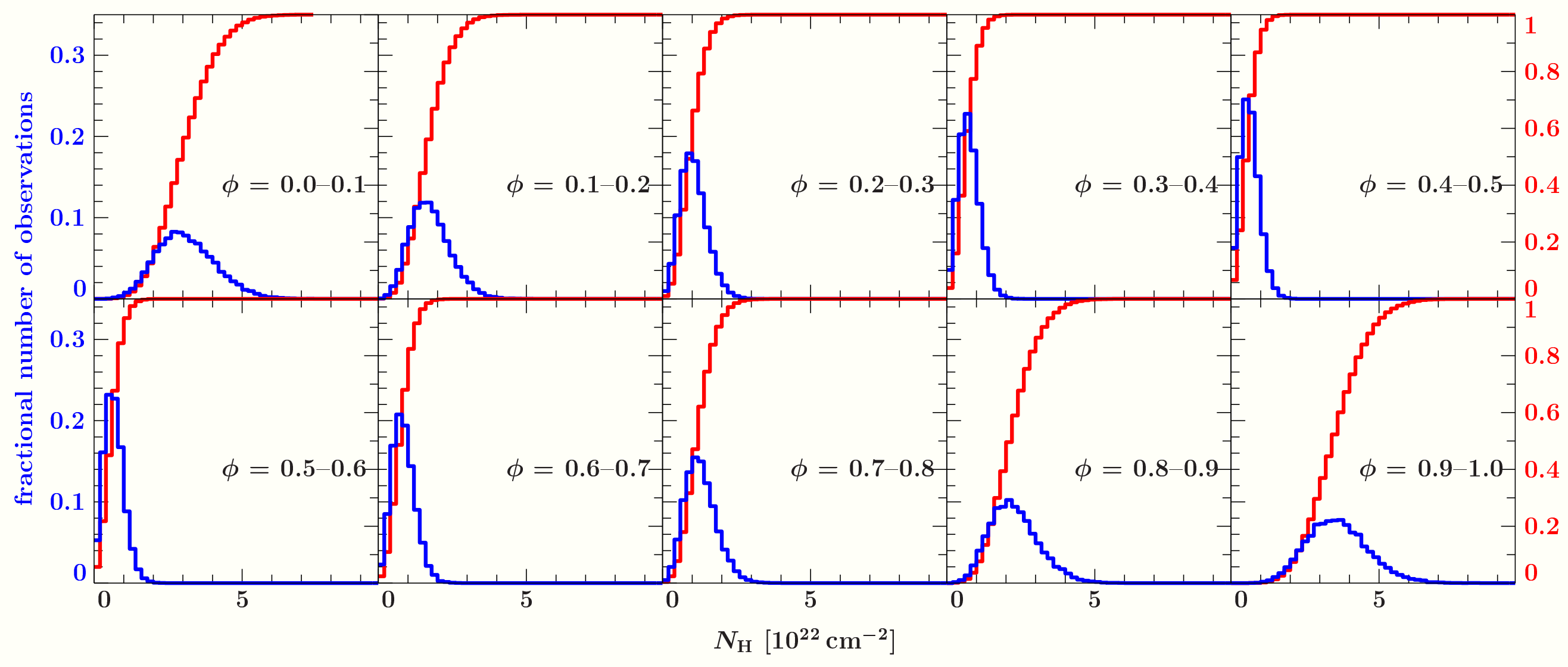

We show (cumulative) histograms of N_H during the hard state of 2006–2010 on the upper figure on the left.
We construct a toy model of the clumpy wind by adapting the clumpy wind simulation engine of Sundqvist et al. 2012 (see also Owocki & Cohen, 2006) to the Cyg X-1/HDE 226868 system parameters. The model does not yet account for the focussed wind properties but treats the wind of HDE 226868 as that of a single star. The tunable parameters of the model are the number of clumps N between $1.2R_*$ and $50R_*$ (R_* radius of HDE 226868), and the terminal clump size far out in the wind, or alternatively the terminal porosity length h_∞ (see Sundqvist et al., 2012). The lower figure above shows a histogram of the N_H values obtained for such a clumpy wind model with $N = 1000$ and $h_\infty \approx R_*$ by adding an X-ray source at the position of the black hole.
We assess whether the models describe the data well by eye and by comparison of the average values and their variances in a given orbital phase range: models with $h_\infty \approx R_*$ are in general agreement with the data, albeit with large uncertainty. $h_\infty \approx 0.1R_*$ or $10R_*$ seems inconsistent with the data. The agreement is best at $\phi_\mathrm{orb} \approx 0.5$; strong deviations are visible at $\phi_\mathrm{orb} \approx 0$ and we interpret them as due to the focussed part of the wind that is not yet included in the clumpy wind models.

Probing the hot gas phase with Chandra (Miškovičová et al., A&A subm.)

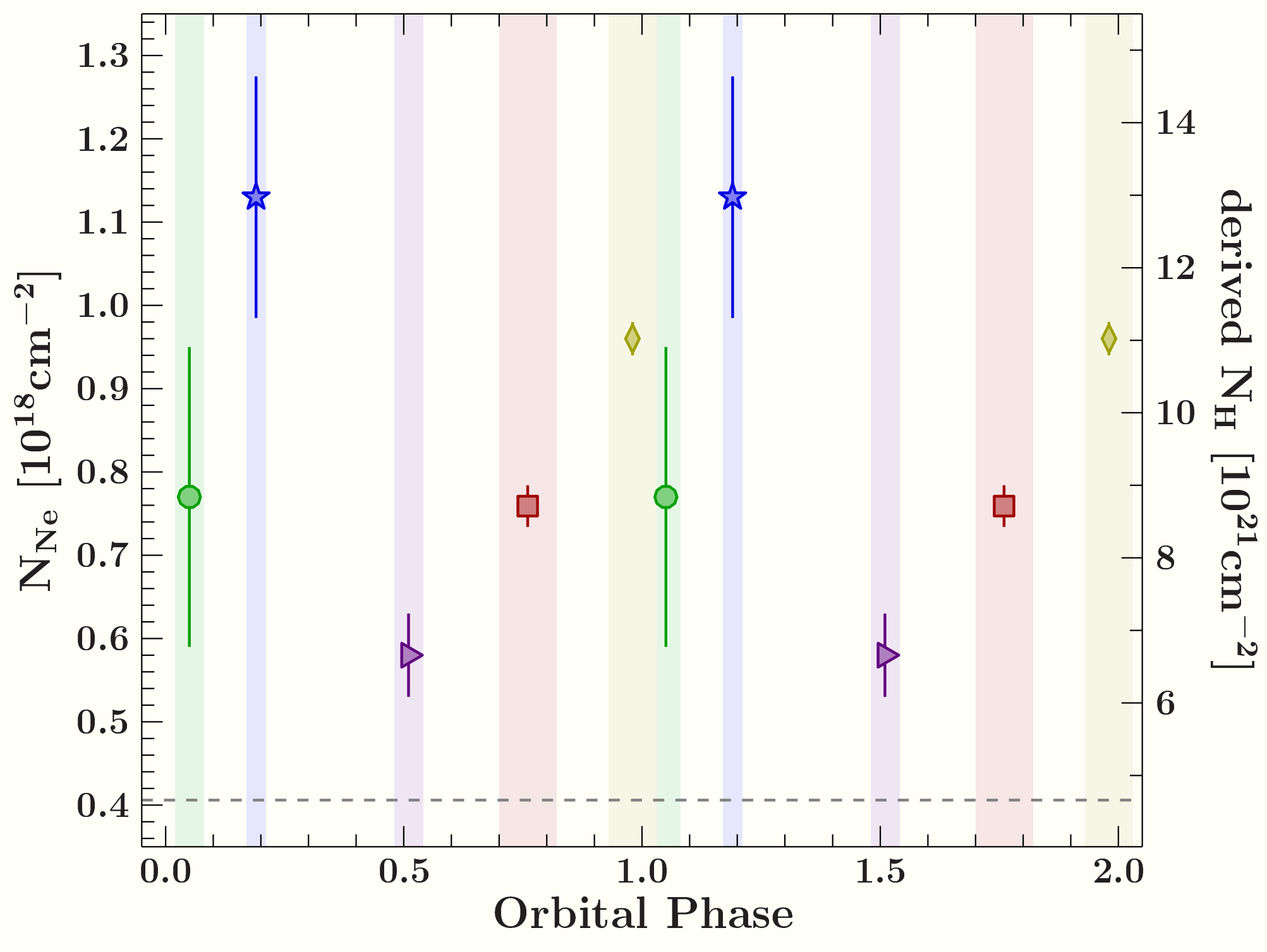

We use all five hard state *Chandra* observations that are shown in the above box and concentrate on the non-dip periods (colored part of lightcurves), i.e., we investigate the hot tenuous gas phase, not the clumps. Modeling N_H from continuum in line-dominated spectra suffers from systematics, thus we measure the optical depth directly at the NeK edge that is visible in all observations used (left figure). The absorption is clearly modulated with orbital phase.
We further fit all absorption lines of an ion simultaneously with a curve of growth approach to obtain the column densities of individual ions, N_i, (not shown), excluding $\phi_\mathrm{orb} \approx 0.5$ where P-Cygni profiles of the lines necessitate a different approach. N_i roughly follow the same trend as N_H.

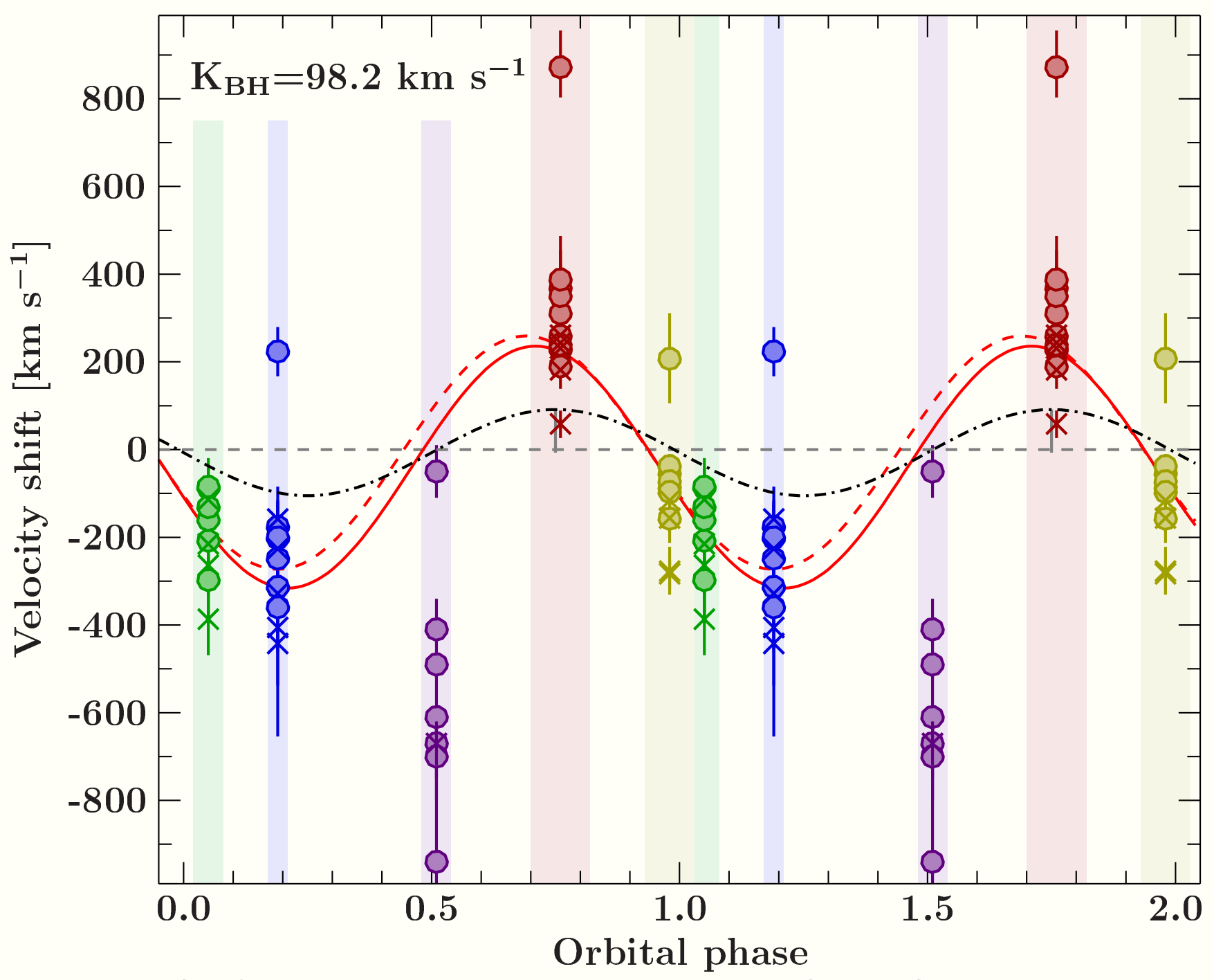

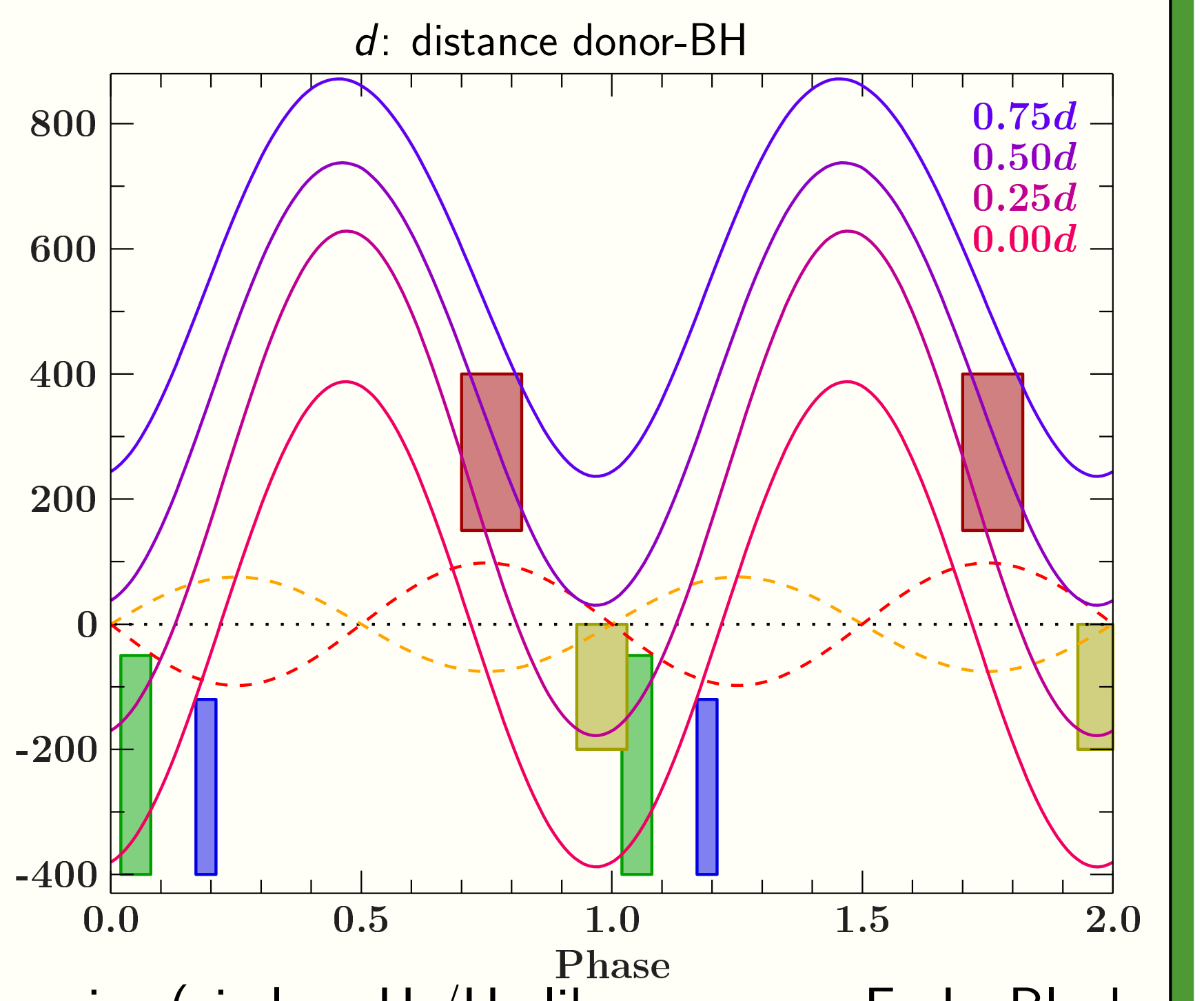

The left figure shows velocity shifts of individual line series (circles: H-/He-like, crosses: Fe L. Black line: radial velocity of BH. Red line: best fit (sine) to all data points. Red dashed line: offset fixed to systemic velocity of BH). Fitting individual line series shows clearly that velocities of different ions are inconsistent with each other and thus hints to a complex ionization structure. The strong blueshift of the weak P Cygni absorption component in $\phi_\mathrm{orb}\sim0.5$ is evidence that the wind has a non-focused part also on the X-ray irradiated side of the companion.
The right figure sets the range of the measured shifts (indicated as boxes) into context with Keplerian velocities of BH (red) and donor (yellow) and the wind velocities projected onto the line of sight as a function of distance from the BH (d: distance donor-BH). The predicted phase shift $\Delta\phi = 0.25$ between BH and wind is not observed. At $\phi_\mathrm{orb}\sim0.0$ velocities are consistent with an origin $\lesssim 0.25d$ from BH. At $\phi_\mathrm{orb}\sim0.75$ is consistent with a slightly larger distance $\lesssim 0.5d$, but this is the brightest observation, i.e., the ionization region is expected to move away from BH. $\phi_\mathrm{orb}\sim0.2$ shows a much higher blueshift than the BH rather than the expected redshift. In the focused wind model this would require a terminal velocities $> 4500\,\mathrm{km\,s^{-1}} \gg\sim 2500\,\mathrm{km\,s^{-1}}$ typically assumed at BH location. However, at this phase the line of sight passes through the "bow shock" of BH (Manousakis, 2011; Blondin and Woo, 1995), a strongly disturbed region where gas obtains a significant non-readial velocity, which at $\phi_\mathrm{orb}\sim0.2$ translates to a high blueshift. Overall the Doppler shifts agree with an origin close to the BH.

References

Blondin, J. M. & Woo, J. W. 1995, ApJ, 445, 889 • Castor, J. I., Abbott, D. C., & Klein, R. I. 1975, ApJ, 195, 157 • Feldmeier, A., et al. 1997, A&A, 322, 878 • Gies, D. R. & Bolton, C. T. 1986, ApJ, 304, 389 • Grinberg, V., et al. 2013, A&A, 554, A88 • Grinberg, V., et al. 2014, A&A, 565, A1 • Manousakis, A. 2011, Thése de doctorat Université de Genève • Oskinova, L. M., et al. 2012, MNRAS, 421, 2820 • Owocki, S. P., et al. 1988, ApJ, 335, 914 • Owocki, S. P. & Cohen, D. H. 2006, ApJ, 648, 565 • Pottschmidt, K., et al. 2003, A&A, 411, L383 • Sundqvist, et al. 2012, MNRAS, 420, 1553 • Wilms, J., et al. 2000, ApJ, 542, 914 • Wilms, J., et al. 2006, A&A, 447, 245 • Xiang, J., et al. 2011, ApJ, 738, 78

Acknowledgments

Support for this work was provided by NASA through the Smithsonian Astrophysical Observatory (SAO) contract SV3-73016 to MIT for Support of the Chandra X-Ray Center (CXC) and Science Instruments; CXC is operated by SAO for and on behalf of NASA under contract NAS8-03060. It was partially completed by LLNL under Contract DE-AC52-07NA27344, and is supported by NASA grants to LLNL and NASA/GSFC. We thank the Bundesministerium für Wirtschaft und Technologie for funding through Deutsches Zentrum für Luft- und Raumfahrt grant 50 OR 1113. We acknowledge funding by the European Community's Seventh Framework Programme (FP7/2007-2013) under grant agreement number ITN 215212 "Black Hole Universe" and by the Bundesministerium für Wirtschaft und Technologie under grant numbers DLR 50 OR 0701 and 50 OR 1113. RHDT acknowledges support from NASA award NNX12AC72G. We acknowledge the support by the DFG Cluster of Excellence Origin and Structure of the Universe and are grateful for the support by MCB through the Computational Center for Particles and Astrophysics (C2PAP). This research has made use of ISIS functions (`isisscripts`) provided by ECAP/Remeis observatory and MIT (`http://www.sternwarte.uni-erlangen.de/isis/`).